

# Solder Metalization Interdiffusion in Microelectronic Interconnects

A. Zribi, R.R. Chromik, R. Presthus, J. Clum, K. Teed, L. Zavalij, J. DeVita, J. Tova, E.J. Cotts  
State University of New York at Binghamton Physics Department  
P.O.Box 6016 Binghamton, NY 13902  
ecotts@binghamton.edu

## Abstract

We investigated Intermetallic compound formation mechanisms and their effect on the integrity of ball grid array Cu/Ni/Au/solder joints integrity were investigated. Substrates with three types of Au plating, and thus three different thicknesses [ Electrolytic (2.6 and 0.75 $\mu\text{m}$ ), Immersion (0.25 $\mu\text{m}$ ), and Selective (0.02 $\mu\text{m}$ ) ] were used. After solder reflow, the solder joints were annealed for up to 1000 hrs at 150°C. Optical and electronic metallography together with Energy Dispersive Spectroscopy were used to locate and identify phases present in the joint for different annealing times. Brittle failure of solder joints was ascribed to the formation of a ternary intermetallic ( $\text{Au}_{0.5}\text{Ni}_{0.5}\text{Sn}_4$ ) at the interface solder/substrate. In the absence of post-reflow thermal aging, only  $\text{Ni}_3\text{Sn}_4$  was observed at the interface and it did not decrease the mechanical reliability of the joint. Tensile-shear stress tests were performed on unaged samples as well as samples aged for 1 hr, 4 hrs and 450 hrs.

## Introduction

The formation of intermetallic compounds (IC's) has always concerned engineers and scientists in the process and design of metallic structures. These compounds tend to be brittle at low temperatures and therefore are a potential cause of failure of metallic systems, since cracks initiate and grow easily in these materials.

Electronic packaging is an area where severe embrittlement problems related to IC's continue to arise. More specifically, premature mechanical failures have been reported in Cu/Ni/Au BGA/solder joints [1]. A number of different IC's have been blamed for the failures including  $\text{AuSn}_4$ . In many cases, Au was implicated as the direct cause of the degradation of the joint quality. In fact, Au is primarily used to protect Ni from corrosion, it dissolves rather fast in molten solder, and has a high solubility [2,3,4]. Depending on the initial thickness of Au, the reflow profile and the posterior thermal history of the sample, the joint microstructure and composition will develop differently. Nevertheless, a number of investigations [1,5] have reported the formation of a  $\text{AuSn}_4$  intermetallic near the Ni/solder interface. This IC is known for its deleterious effect on the mechanical reliability of solder joints. This binary Au-Sn intermetallic is a weak, brittle compound that degrades the thermal fatigue life of the joint when present in high concentrations [5].

The concentration of Au in the joint is therefore important, since it dictates how thick an IC can possibly grow. Since the interest in studying the influence of alloying Pb-Sn solder with Au started, a whole range of Au concentrations has been explored by several investigators [3,4,5]. According to these

works, Au has a propensity to embrittle solder joints within a range of concentration that extends from 2 to 7 wt%. Other investigators [1] referenced a rule of thumb value of Au concentration of 3 wt% beyond which the solder joint degrades considerably. The present work concerns a failure mechanism due to a Au IC for Au concentrations as low as 0.2 wt%.

In publication [1], the authors ascribed the brittle failure of BGA /Au/Ni/Cu joints to migration of  $\text{AuSn}_4$  from the bulk of the solder joint, where it nucleated during reflow, to the interface adjacent to the  $\text{Ni}_3\text{Sn}_4$  intermetallic after thermal aging. The coexistence of these two phases with poor adhesion properties to each other was held responsible for the observed deterioration of the joint. These investigators reported a detrimental effect of  $\text{AuSn}_4$  on the bending strength of BGA assemblies where breakage energies dropped considerably due to presence of  $\text{AuSn}_4$  at the interface solder-substrate pads.

Our early investigations showed that  $\text{AuSn}_4$  does not form in our samples, and rather a ternary Au-Ni-Sn compound grew at the interface. In addition, the aforementioned works emphasized the effect of different Au concentrations on the mechanical properties of the bulk solder, whereas we focused our work on developments of the interfacial microstructure and morphology and its effect on the joint reliability.

We conducted our investigation in an attempt to understand the mechanism driving the formation of Au IC's at the Ni/solder interface. Different substrates from two different vendors, with three Au/Ni plating categories (electrolytic, immersion and selective) and hence thickness, were used to prepare the BGA packages. A special interest was also devoted to explaining how the presence of these phases considerably reduces the toughness and the ductility of the joints.

## Samples preparation

FR4 substrates from two different vendors were used to make the specimens for this study. The printed circuit boards were populated with eutectic solder spheres arranged in one row around the perimeter of the board layout. After placing the balls with a placement machine, the boards were sent to a reflow oven. The reflow procedure is carried out according to vendor recommendations and the reflow profile is displayed in **Figure 1**.

The samples were subsequently sealed in argon and annealed in a convection oven at 150°C for up to 1000h. After annealing, the samples were cross-sectioned and prepared for inspection.

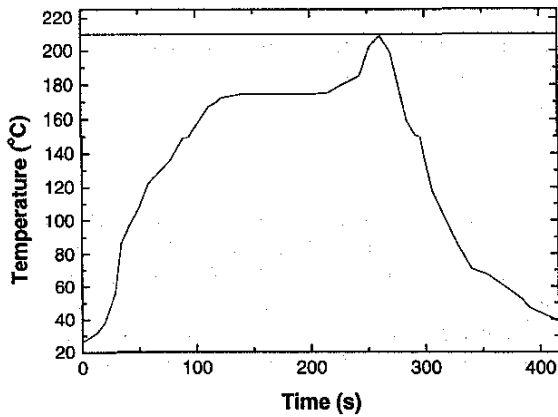


Figure 1: Temperature-reflow profile

I. Equilibrium Phase diagram analysis

A. Dissolution of Au and Ni in molten solder

When eutectic Sn-Pb solder is reflowed on Ni/Au-coated copper pads, interfacial dissolution reactions occur. This dissolution is controlled mainly by three parameters: temperature, solubility of the solute at the operating temperature, and its initial concentration. These parameters, together with experimental measurements, provided for sufficient data to estimate the dissolution rate of Au and Ni in molten solder.

A published paper [2] established that dissolution rates of both Ni and Au in eutectic solder follow an Arrhenius relationship. Although the investigation used thin wires of Ni and Au in a rather large volume of molten solder, the paper reported good agreement with similar data obtained for thin films. By extrapolating the data provided in [2] towards lower temperatures (Figure 2), both Ni and Au dissolution rates were estimated to ( $R_{Ni}=0.002 \mu\text{m/s}$  and  $R_{Au}=1.33 \mu\text{m/s}$ ) at 209°C (the reflow temperature in our case).

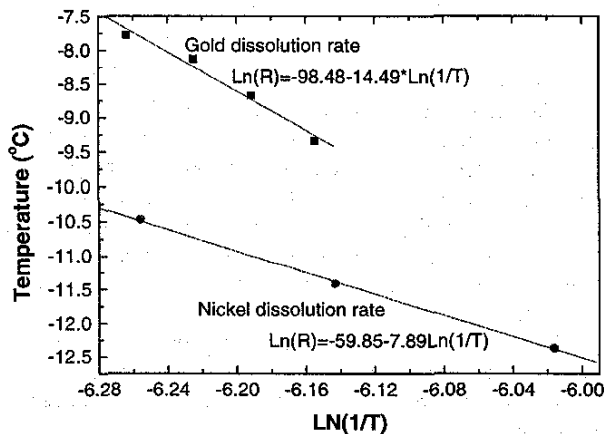


Figure 2: Dissolution rate of Au/Ni in eutectic solder versus temperature

Figure 3 and Figure 4 show sections of the ternary phase diagrams of Pb-Sn-Au and Pb-Sn-Ni respectively. From these diagrams the solubility limit of Au and Ni in the molten eutectic solder are estimated to 3-4 at % for Au and about  $10^{-5}$  at % for Ni.

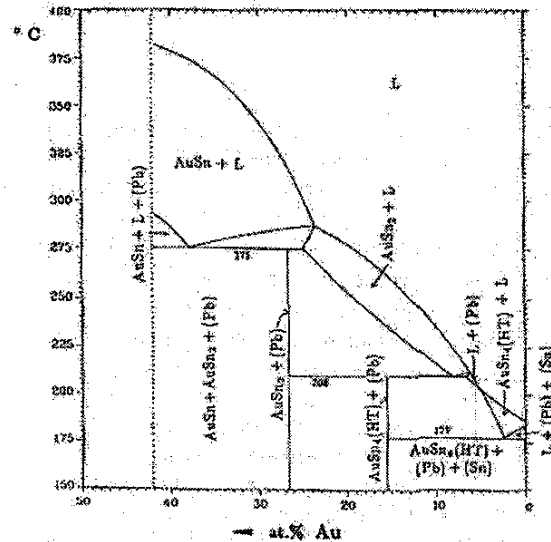


Figure 3: Binary section of the ternary phase diagram Au-Sn-Pb

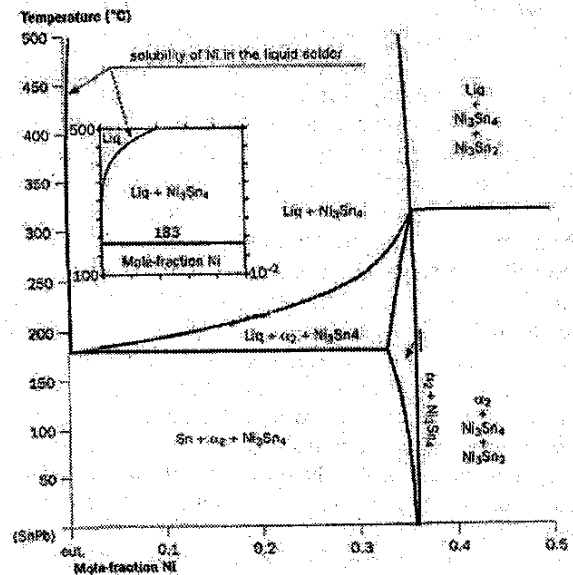


Figure 4: Binary section of the ternary phase diagram Ni-Sn-Pb

As the dissolution rate of Au exceeds that of Ni by almost three orders of magnitude, and the solubility of Au that of Ni by five orders of magnitude, the thin Au layer is expected to disappear rather fast during reflow, exposing Ni for quite a long time to the action of the molten solder.

In order to find out the thickness of Au and Ni for the three plating categories, a Scanning Auger Microprobe was used to analyze a  $60\mu\text{m} \times 50\mu\text{m}$  area on each pad with a 3kv electron beam. The surface was exposed to series of five 1-

minute sputters (with 3 keV Ar ions at a rate of 0.07 nm/s) separated by surface scans. The resulting concentration profiles of the detected elements were plotted in concentration versus depth curves. The Au and Ni layer thicknesses are reported in **Table 1**.

depth	Electrolytic (1)	Electrolytic (2)	Immersion	Selective
Au ( $\mu\text{m}$ )	2.6	0.75	0.25	0.02

**Table 1:** Thickness of the Au and Ni layer versus plating technology.

Assuming that the molten solder perfectly wets the Au surface, it would take less than a second (0.5 s) to dissolve the thickest layer of Au (electrolytic) with the aforementioned dissolution rate of 1.3  $\mu\text{m/s}$ . The concentrations of Au and Sn in molten solder, given in **Table 2**, are estimated based upon the average dimensions of the BGA solder balls measured by a calliper. Within the time afforded by the reflow process, the Ni-layer will be therefore exposed to the molten solder for approximately 35 s. This time accounts for the wetting time, which according to the literature would be approximately 10 s [6].

at % (in molten solder)	Au	Ni (less than)
Electrolytic 1	0.34	$10^{-5}$
Electrolytic 2	0.1	$10^{-5}$
Immersion	0.031	$10^{-5}$
Selective	0.0027	$10^{-5}$

**Table 2:** Concentrations of Au and Ni in the molten solder

The Ni dissolution process will continue until the liquid solder saturates. At this time the most Sn-rich intermetallic compound precipitates out of the solution and consumes the Ni dissolved up to that point. In agreement with the binary section of the ternary phase diagram Pb-Sn-Ni (**Figure 4**) the precipitating intermetallic is  $\text{Ni}_3\text{Sn}_4$ . As all physical systems undergoing phase transformations attempt to reduce the surface energy barrier for the new phase to generate, the nucleation of this phase is expected to occur upon a pre-existing interface. The molten solder-Ni interface being the only available in our system,  $\text{Ni}_3\text{Sn}_4$  is very likely to nucleate and subsequently grow on top of the Ni layer.

A layer of Ni of only 0.0048  $\mu\text{m}$  is expected to dissolve, given the extremely low solubility limit of Ni in molten eutectic solder and dimensions of the BGA spheres (**Figure 5**). The dissolution process will therefore go on for only 2.4 of the 35 seconds afforded by the reflow stage, and hence the remaining time will allow  $\text{Ni}_3\text{Sn}_4$  to grow from the Ni layer. The phase growth naturally involves both liquid and solid state reactions as the eutectic is kept in a liquid state and the emerging solid phase is adjacent to the solid layer of Ni.

The reaction constant for the solid/liquid state reaction between Ni and Sn is estimated to  $3.2 \times 10^{-10} \text{ cm}^2/\text{s}$  at 209°C

[8]. Therefore, a  $\text{Ni}_3\text{Sn}_4$  intermetallic layer of approximately 1  $\mu\text{m}$  in thickness is expected to grow at the interface during reflow.

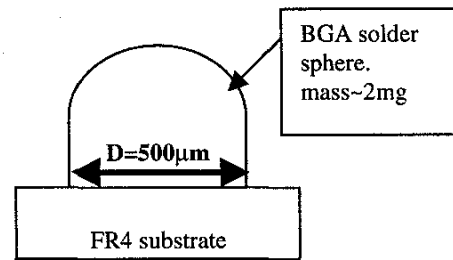


**Figure 5:** Geometrical configuration of a typical sample

While Ni-Sn intermetallics are expected to form during solder reflow, Au remains in solution with Sn while the system is above the liquidus temperature. Considering the very low Au solubility in the Pb-rich phase of the solder, most of the dissolved Au is expected to remain in the Sn-rich phase. At lower temperatures, this configuration is metastable. The Au atoms initially dispersed in the Sn matrix will attempt to form new phases as the solubility limit drops from (3-4at%) at the reflow temperature to (less than 0.01 at%) at room temperature. However, as the temperature decreases the mobility of Au atoms decreases. The diffusion coefficient of Au in pure Sn has been estimated by previous studies [8] to be  $1.25 \times 10^{-14} \text{ cm}^2/\text{s}$  at room temperature. Accordingly little or no gold redistribution occurs at room temperature.

### B. Crystallization analysis

We first examine the changes that occur for a single composition, homogeneous liquid as a function of temperature under equilibrium conditions. These conditions are not necessarily attained in our experiment since, to simulate the production conditions, the system was rapidly cooled. Nevertheless, consideration of equilibrium products helps us to understand the actual, observed state of the sample after rapid cooling.

The initial concentrations of Au, Pb and Sn is given in **Table 3** for the three types of Au plating. The concentration of Au is assumed to be homogeneous [2,4] in the following discussion.

at % (in molten solder)	Electrolytic (1)	Electrolytic (2)	Immersion	Selective
Au	0.34	0.1	0.031	0.0027
Sn	74.4	74.58	74.6	74.7
Pb	25.26	25.32	25.37	25.29

**Table 3:** Atomic concentration of Au, Sn and Pb in molten solder before cooling.

Considering that Au-Sn intermetallic compounds were found both at the interface and in the outermost shell of solder balls reflowed on thick Au substrates [4], many modeling works [2] assumed a homogenization of the liquid solder by convection-diffusion. Therefore, we will carry through these analysis under the same assumption.

When a homogeneous liquid of a fixed composition cools down, it remains liquid until we reach the liquidus surface. The first solid crystallizes after the temperature goes slightly below the liquidus temperature. As the arrows on the phase diagram shown in **Figure 6** point to falling temperatures, the crystallization path starting at the initial compositions will terminate at the eutectic  $E_2$ .

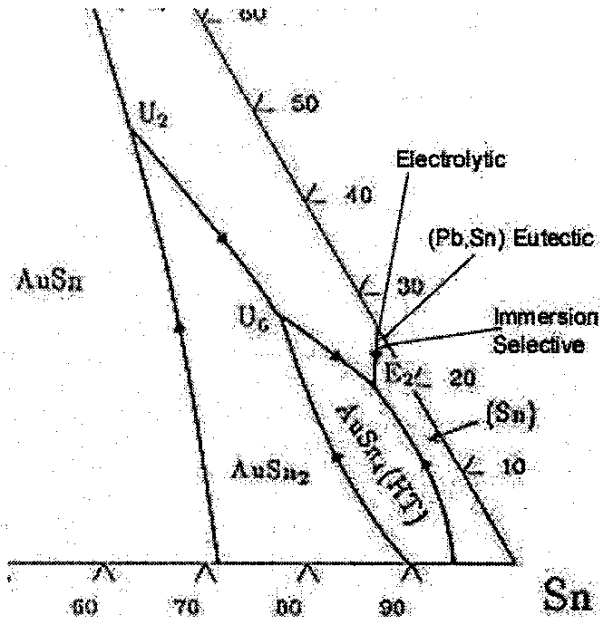
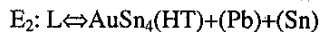


**Figure 6:** Liquidus projection of the ternary phase diagram

The initial composition of the solution falls in the Sn primary crystallization field for all our samples as shown in **Figure 6**. Therefore, the first solid to form from the melt is a Sn-rich phase. This Sn depletion might yield a typical flower shaped morphology of the solidifying phase.

As the temperature of the system declines along the boundary line  $e_2-E_2$ , eutectic solder continues to solidify and hence the remaining liquid gets enriched in Au regardless of the sample category. This process will continue until the eutectic temperature  $T_{E2}=176^\circ\text{C}$  is reached. Eventually below the eutectic temperature, the material is completely solid as a result of the eutectic reaction:



Henceforth, we established that when starting our initial liquid compositions in Au are assumed to be homogeneous,  $\text{AuSn}_4$  will only nucleate if equilibrium conditions are fulfilled throughout the cooling process. Nonetheless, such conditions require a slow cooling rate, which is probably not provided in our experiments, consequently  $\text{AuSn}_4$  is not likely to form after reflow in our samples.

## II. Phase identification and intermetallic growth mechanisms

Because the macroscopic properties of a material are directly related to its microstructure, we conducted microstructural investigations of our samples. Optical and electron metallography were used to examine cross-sectioned samples. One of the objectives was to determine the effect of thermal aging on the microstructure. Thus, all samples were aged at  $150^\circ\text{C}$  for 0.5hrs, 1hr, 4hrs, 9hrs, 40hrs, 150hrs, 450hrs and examined together with unaged specimens.

Five distinct phases were commonly observed in all samples, regardless of the aging time. These phases were identified by EDS (Energy Dispersive spectroscopy) spectra, along with their spatial location in the sample, to be Cu, Ni,  $\text{Ni}_3\text{Sn}_4$ , and the Sn-rich and the lead-rich phases of the solder, as shown in **Figure 7**. After 150 h of thermal aging, some of the electrolytic samples exhibited the presence of a new phase at the interface, which was identified as a Ni-Au-Sn ternary phase. This manifest phase showed up in the immersion samples as well, but only after 450h of annealing at  $150^\circ\text{C}$ .

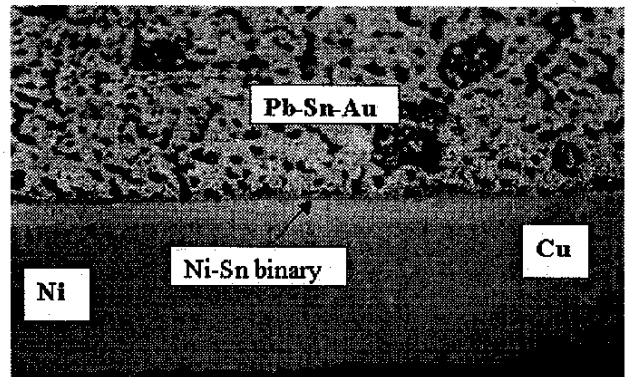


**Figure 7:** Optical micrograph 1000X. Interfacial microstructure of an as-reflowed joint

The interfacial phase, presumably a product of the reaction between molten solder and the substrate pad, grows thicker during the aging process. The growth of this ternary phase adjacent to the previously formed binary  $\text{Ni}_3\text{Sn}_4$  is a potential limitation to the growth of the latter.

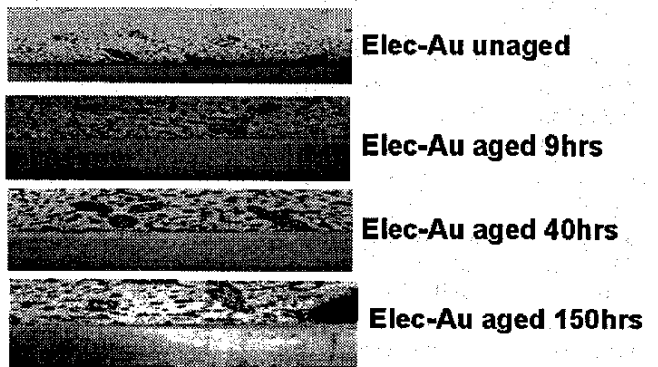


**Figure 8:** Optical micrograph 1000X. Ni-Sn intermetallic growth at the interface solder-Ni

The thickness of the Ni-Au-Sn layer has been measured as a function of the aging time for every sample using EDX (Energy Dispersive X-ray analysis) linescans and optical micrographs at 1000X magnification. In addition **Figure 8** features the development of the morphology of this phase from separated-islands.

**Figure 9** shows a flower-shaped black phase. This Pb-rich phase, as confirmed by EDX line scans **Figure 10**, tends to form in all samples. As similar trends were observed in eutectic solder-cu systems [7], the morphology of this phase could be ascribed to Sn depletion from the eutectic solder. This could occur if Sn reacts preferentially with another metal.

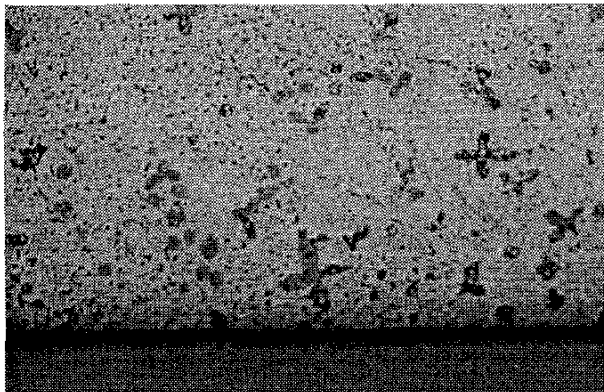


**Figure 9:** Optical micrograph 1000X of an electrolytically plated specimen showing the flower-shaped phase.

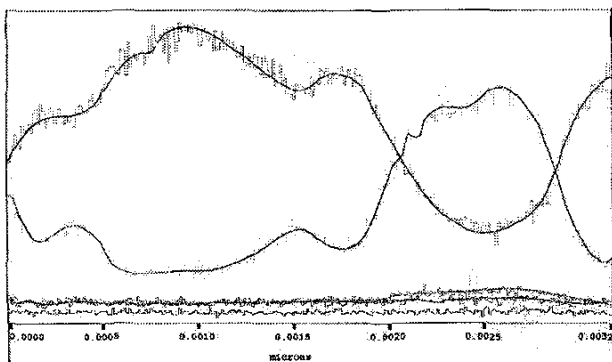


**Figure 10:** EDX linescan across the flower shaped phase

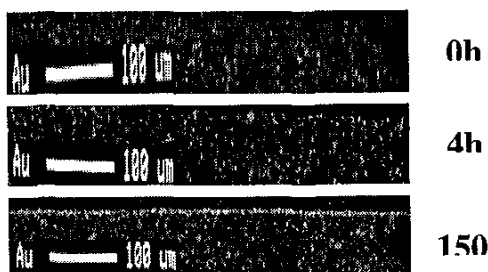
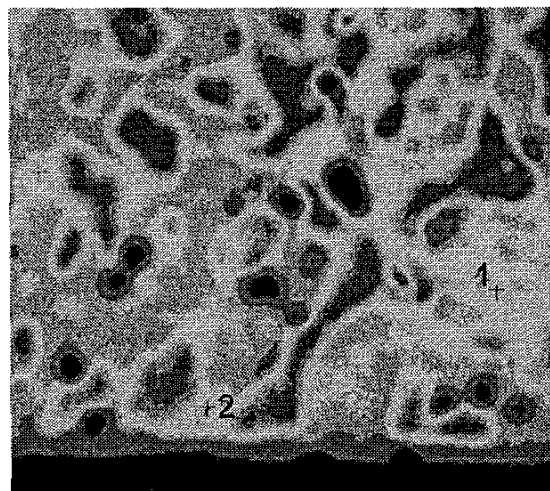


**Figure 11:** X-ray Au maps acquired from the interface solder-pad metallization for three electrolytic samples respectively unaged, aged 4hrs and aged 150hrs at 150°C.

EDS maps and linescans acquired from different locations provided the chemical composition of the physically identified phases. As suggested in the equilibrium phase diagram analysis section,  $Ni_3Sn_4$  forms during reflow at the interface. The composition of this phase was determined by x-ray semi-quantitative analysis (ZAF) using a microprobe. The approximate atomic composition of this binary intermetallic according to this analysis is: 44 at% Ni and 56at% Sn, which is within experimental error of the stoichiometric alloy,  $Ni_3Sn_4$ .

As the samples age at 150°C for longer times, Au atoms are able to diffuse appreciable distances throughout the Sn-rich phase of the solder. A combination of energetics and kinetics drives Au atoms to migrate towards the interface solder- $Ni_3Sn_4$ -Ni to form a ternary intermetallic compound (Au,Ni)-Sn, leading the system to increase its stability. **Figure 11** illustrates this mechanism. It shows three x-ray maps belonging to identical samples from a metallurgy standpoint (electrolytic) aged respectively at 0h (as reflowed), 4h and 150h. In these maps no Au could be viewed until 150h of aging at 150°C. Ultimately Au shows up at the interface, between the solder and the  $Ni_3Sn_4$  layer. Microchemical analysis inside this phase **Figure 12** revealed the average composition of this compound to be approximately  $(Au_{0.5}Ni_{0.5})Sn_4$ .



Atomic Ratio:	Group:	
Element:	1	2
P	--	--
Au	8.5387	8.6722
Sn	80.3010	81.0496
Ni	11.1603	10.2782
Total:	100.0000	100.0000

**Figure 12:** SEM backscattered electrons image of the showing the  $(Au_{0.5}Ni_{0.5})Sn_4$  phase at the interface. ZAF analysis at two different spots are included in.

Similar trends were observed occasionally in a few of the immersion samples. No Ni-Au-Sn ternary IC growth was noticeable in the case of the selective Au plating, most likely because of the very low initial Au concentration.

### III. Kinetics for the growth of Intermetallic compounds at the interface

The thickness of the intermetallic layer growing at the interface was measured as a function of aging time using Scanning Electron Microscopy, optical micrographs, and the EDS linscans performed perpendicularly across the interface. The solid state reaction constant was calculated based upon this data for each category of sample. For one-dimensional growth, the solid state reaction constant of  $\text{Ni}_3\text{Sn}_4$  is estimated to average  $2 \times 10^{-14} \text{ cm}^2/\text{s}$  at  $423^\circ\text{K}$ .

The calculated reaction constant is two orders of magnitude smaller than values determined in previous works [8] by DSC (Differential Scanning Calorimetry) analysis performed on stoichiometric pure Sn-pure Ni couples. The latter studies showed that Ni reacts with Sn in solid state, and the reaction constant was evaluated to be  $1.58 \times 10^{-12} \text{ cm}^2/\text{s}$  at  $150^\circ\text{C}$ .

The presence of lead in the system is expected to slow down the growth kinetics of the intermetallic layer, as has previously been observed in either systems.

### IV. Effect of intermetallic growth on the mechanical integrity of the joints

Tensile shear tests were undertaken to study the systematics of brittle failure. Figure 13 displays the test configuration. The BGA packages were diced and cut into solder-ball rows. These rows were attached to a fixture and subjected to compressive stresses using an INSTRON tensile-testing machine. The force-displacement curves generated for the tested balls were used to determine the type of failure, the breakage energy and the strength of the joint.

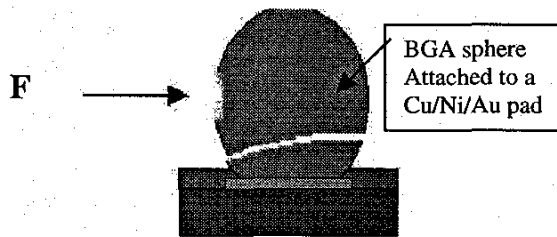


Figure 13: Mechanical test configuration.

Typically joints failed in what was termed to be either a "ductile" or a "brittle" manner. Figure 14 and Figure 15 respectively show typical displacement curves of a ductile and a brittle type joint. Figure 14 belongs to a non-aged specimen while Figure 15 belongs to a specimen aged for 150hrs at  $150^\circ\text{C}$ . Ductile fractures were associated with failure in the solder ball, while brittle fractures were associated with failure at the Ni/solder interface.

The tensile strength of the joint for the unaged samples exceeded that of the aged samples. The drop of joint strength and ductility is perceptible in terms of breakage energy of the joint (the integral of the area under the force-displacement curve). The breakage energy is plotted versus anneal time in Figure 16.

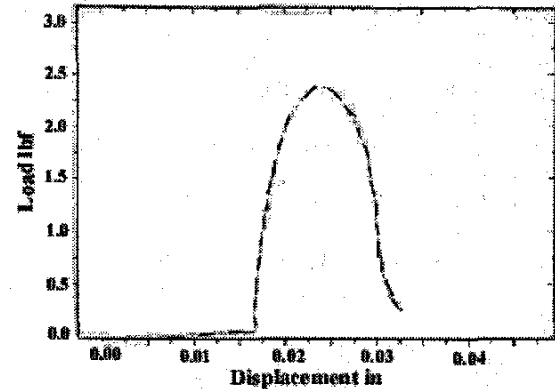


Figure 14: Load-displacement curve for an unaged sample

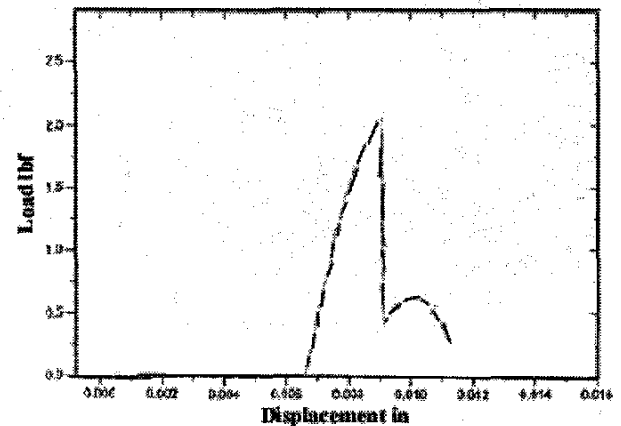


Figure 15: Load-displacement curve for a specimen aged 150hrs at  $150^\circ\text{C}$

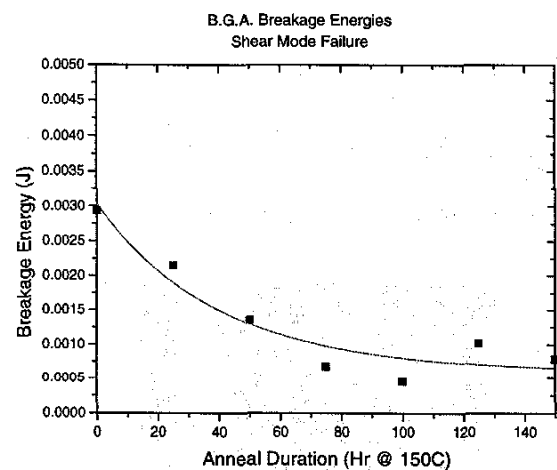
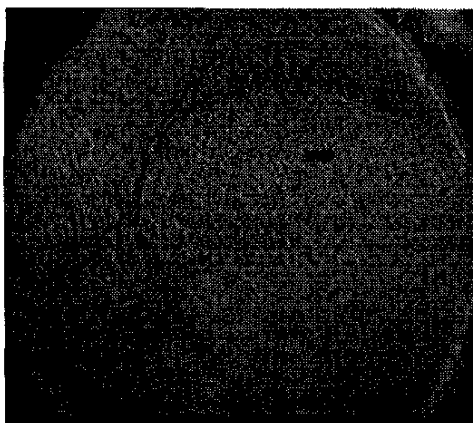


Figure 16: Effect of the annealing time on breakage energy of BGA Solder balls

Observation of the fracture surface of broken electrolytic sample under the microscope reveals a flat surface Figure 17 which indicates a brittle failure in contrast with a cone-shaped

fracture surface **Figure 18** that would correlate with a ductile fracture selective sample.



**Figure 17** Optical micrograph 200X of the fracture surface of an electrolytic sample.



**Figure 18** Optical micrograph 200X of the fracture surface of a selective sample.

#### Conclusion

A ternary intermetallic phase  $(Au_{0.5}Ni_{0.5})Sn_4$  was observed to grow at the  $Ni_3Sn_4$ /solder interface upon annealing. This phase grows from the  $Ni_3Sn_4$  binary intermetallic viewed at the interface solder-Ni after solder reflow. The presence of  $(Au_{0.5}Ni_{0.5})Sn_4$  decreases the toughness of the joint. The determination of the stoichiometry of the phase  $(Au_{0.5}Ni_{0.5})Sn_4$  provides some understanding of why the phase grew at the  $Ni_3Sn_4$ /solder interface, as only at this interface were Sn, Au and Ni all readily available.

#### Acknowledgments

This research was funded The Integrated Electronics Engineering Research Center (IEEC) located in the Watson School at Binghamton University. The IEEC receives funding from the New York State Science and Technology Foundation, the National Science Foundation and a consortium of industrial members.

We'd like to thank Ms. Susan Pitely for her efforts in helping us edit and prepare this paper for submission.

#### References

1. Mei, Z. et al, "Brittle Interfacial Fracture of PBGA Packages Soldered on Electroless Ni/Immersion Au", Hewlett-Packard Company
2. Bader, W. G., "Dissolution of Au, Ag, Pd, Pt, Cu and Ni in a Molten Sn-Lead Solder", *Welding Journal: Research supplement*, 48(12)(1969) 551s-557s.
3. Kramer, P.A. et al, "The Effect of Low Au Concentrations on the Creep of Eutectic Sn-Lead Joints", *Metallurgical and Materials Transactions A*, Vol.25A, June 1994, pp. 1249-1255.
4. KIM, P.G. et al, "Fast Soldering Reactions On Au Foils", Materials Research Society, *Symposium Proceedings*, Vol.445, 1997, pp.131-136.
5. Ferguson, M. E. et al, "Manufacturing Concerns When Soldering with Au Plated Component Leads or Circuit Board Pads", *IEEE Transactions on Components, Packaging, and Manufacturing Technology-Part C*, Vol. 20, No. 3, July 1997, pp. 186-193.
6. Yost, F.G. et.al., *The Mechanics of Solder Alloy WetSng and Spreading*, Van Nostrand Reinhold, New York, 1993.
7. Kim, H. K et al, "Morphology of instability of the wetSng tips of eutectic SnBi, eutectic Sn-Pb, and pure Sn on Cu", Materials Research Society, Vol. 10, No.3, July 1994, pp.497-504.
8. Chromik, R. R., "The Thermodynamics and Kinetics of Solid State Reactions In The Pd-Sn System", Masters Thesis SUNY at Binghamton, 1996.
9. Ohriner, E. K., "Intermetallic Formation in Soldered Copper-Based Alloys at 150°C to 250°C.", *Welding Journal: Research supplement*, July 1987, pp.191-s/202-s.